

CHAPTER 5

ANALYSIS OF CORONARY CIRCULATION: A BIOENGINEERING APPROACH

GHASSAN S. KASSAB

Department of Bioengineering, University of California, San Diego

1. Introduction

The coronary blood circulation supplies the heart with oxygen and nutrients and removes its waste products. The hemodynamics of the coronary circulation reveal a number of interesting phenomena such as phasic arterial inflow and venous outflow, spatial and temporal flow heterogeneity, the existence of significant vascular compliance and zero-flow pressure, and autoregulation to mention just a few (see recent review by Hoffman and Spaan, 1992). In order to understand such a complex system, it is necessary to analyze each component separately before synthesizing the whole system. In order to initiate the analysis, we consider the simplest possible situation: steady state blood flow in the diastolic, maximally vasodilated state of the coronary vasculature. The effects of systole, vasoactivity and time-varying boundary conditions will be added to the model once a foundation is established using the engineering approach.

In a bioengineering approach to coronary blood flow analysis, one should use the vascular geometry and branching pattern, mechanical properties of the coronary vessels (arteries, capillaries and veins), and rheology of blood in the coronary vasculature, apply the basic laws of physics to write down the governing equations and specify the appropriate boundary conditions, and solve the boundary-value problems. To date, only two organs have been subjected to such detailed analysis. One organ is that of the cat lung (Zhuang *et al.*, 1983; Fung, 1997) and the other is the Spinotrapezius muscle in the rat (Schmid-Schoenbein, 1986). Recently, a full set of data describing the branching pattern and vascular geometry of the entire porcine coronary vasculature, from arteries to capillaries and veins, in the diastolic, maximally vasodilated state has been obtained in our laboratory (Kassab *et al.*, 1993a, 1994, 1994b, 1997a).

In this chapter, I will briefly review the morphometric data of the coronary vasculature and illustrate some of its hemodynamic applications. I will also consider the mechanical properties of the coronary vessels and demonstrate the interaction of blood flow and vessel elasticity in formulating a new pressure-flow relationship for the coronary blood vessels.

2. Innovations in Morphometry of Coronary Vasculature

We have added four new innovations to morphometry: the Diameter-Defined Strahler ordering system for assigning the order numbers of the vessels, the distinction between series

and parallel vessel segments, the connectivity matrix to describe the asymmetric branching pattern of vessels, and the longitudinal position matrix to describe the longitudinal position of daughter vessels along the length of their parent vessels. These innovations were used to study the anatomy of the coronary vasculature in the pig and have yielded the *first complete* set of morphometric data on the coronary arteries (Kassab *et al.*, 1993a, 1997a), capillaries (Kassab and Fung, 1994) and veins (Kassab *et al.*, 1994b) in health as well as that of arterial remodeling in right ventricular hypertrophy (Kassab *et al.*, 1993b). Now that the porcine coronary morphometric data base is complete, we are beginning to demonstrate some of its applications (Kassab *et al.*, 1994a, 1997b and Kassab and Fung, 1995; see accompanying manuscript).

3. Anatomy of the Coronary Vasculature

The heart muscle is perfused via two major coronary arteries: the right coronary artery (RCA) and the left common coronary artery (LCCA). In the porcine, LCCA is a short segment (1–2 mm) which bifurcates into the left anterior descending (LAD) artery and left circumflex (LCx) artery. Figure 1 shows a cast of the LAD artery made from silicone elastomer while Fig. 2 shows examples of the branching pattern of intramural arterioles and venules (Kassab *et al.*, 1993a and Kassab *et al.*, 1994b).

There are two routes by which coronary venous flow returns to the heart. In one route, blood flows from the great cardiac vein, the posterior vein of the left ventricle, the posterior interventricular vein, the oblique vein of Marshall, and anterior cardiac vein into the coronary sinus on the epicardial surface and empties into the right atrium. In another route, blood flows through the smallest cardiac veins of Thebesius to the endocardial surface and drains directly into the heart chambers (predominantly into the right ventricle). The branching pattern of the porcine coronary arteries and endocardial veins are tree-like (Kassab *et al.*, 1993, 1994b), but the coronary capillary blood vessels have a non-tree-like topology (Kassab and Fung, 1994). Arcades are found at the epicardial surface connecting the sinusal veins



Fig. 1. Cast of porcine left anterior descending artery. Scale is 1 cm. From Kassab *et al.* (1993a), by permission.

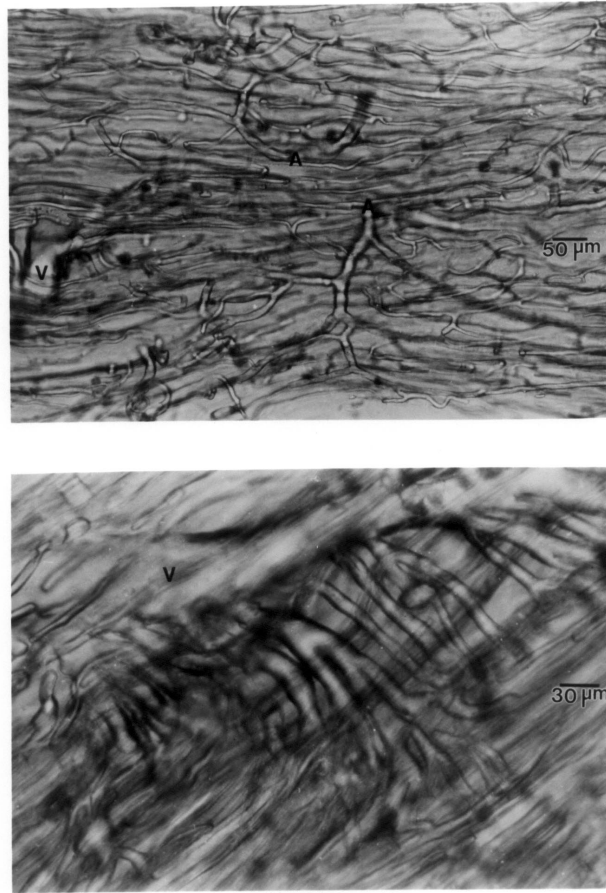


Fig. 2. Photomicrographs of arteriole (A) and venule (B) in the porcine left ventricle. From Kassab *et al.* (1993a, 1994b), by permission.

and at the endocardial surface connecting Thebesian veins (Kassab *et al.*, 1994b). There are also connections between the sinusal and Thebesian veins.

4. Mathematical Description of Coronary Arterial and Venous Trees

First, the capillary blood vessels are defined as vessels of order zero. The smallest arterioles supplying blood to the capillaries are assigned an order number of 1. The smallest venules draining the capillaries are assigned an order number of -1 . When two arterioles of order 1 meet, the confluent vessel is given an order number 2 if its diameter exceeds the diameters of the order 1 vessels by an amount specified by a set of formulas or diameter criterion (Kassab *et al.*, 1993a), or remain as order number 1 if the diameter of the confluent is not larger than the amount specified by the formulas. When an order 2 artery meets another order 1 artery, the order number of the confluent is 3 if its diameter is larger by an amount specified by the diameter criterion, or remains at 2 if its diameter does not increase sufficiently. This process is continued until all arterial segments are arranged in increasing diameter and assigned the order numbers $1, 2, 3, \dots, n, \dots$. Similarly, the veins are assigned

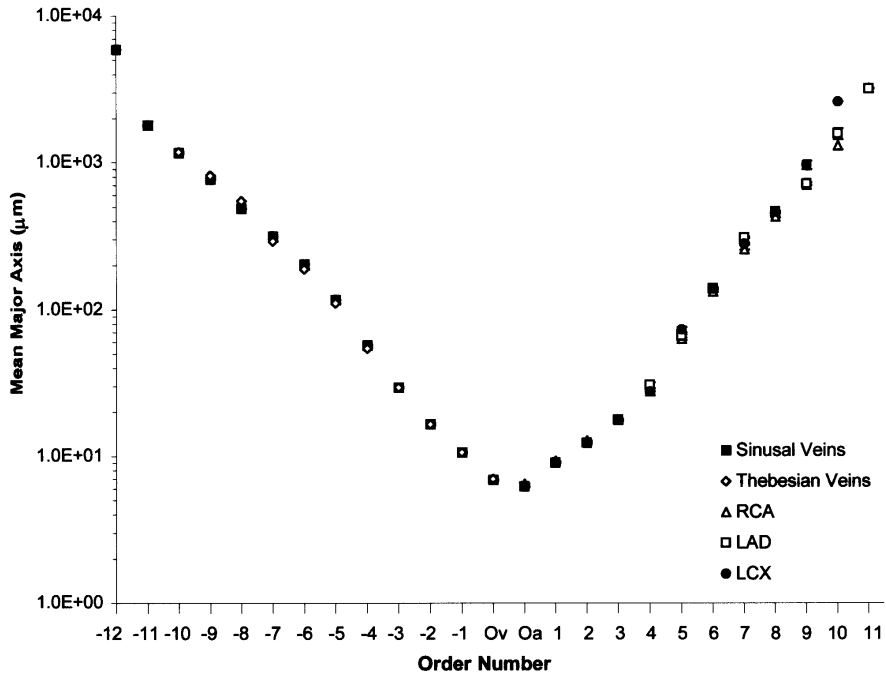


Fig. 3. Relationship between the mean length of the major axes of vessel elements in successive orders of vessels and order number of vessels in the porcine RCA, LAD, LCx, Thebesian and Sinusal Veins. From Kassab *et al.* (1993a, 1994b), by permission.

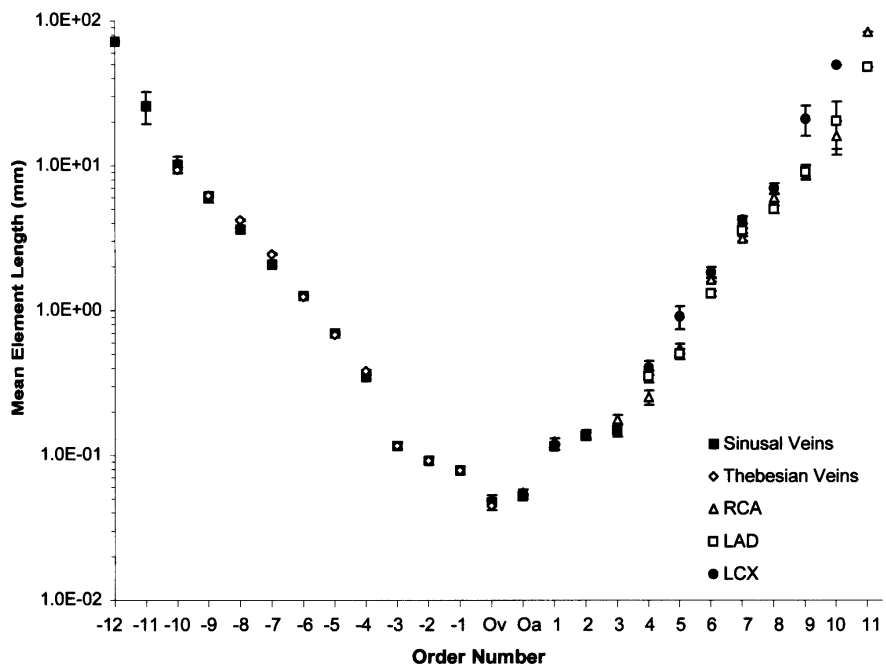


Fig. 4. Relationship between mean length of vessel elements in successive orders of vessels and order number of vessels in the porcine RCA, LAD, LCx, Thebesian and Sinusal Veins. From Kassab *et al.* (1993a, 1994b), by permission.

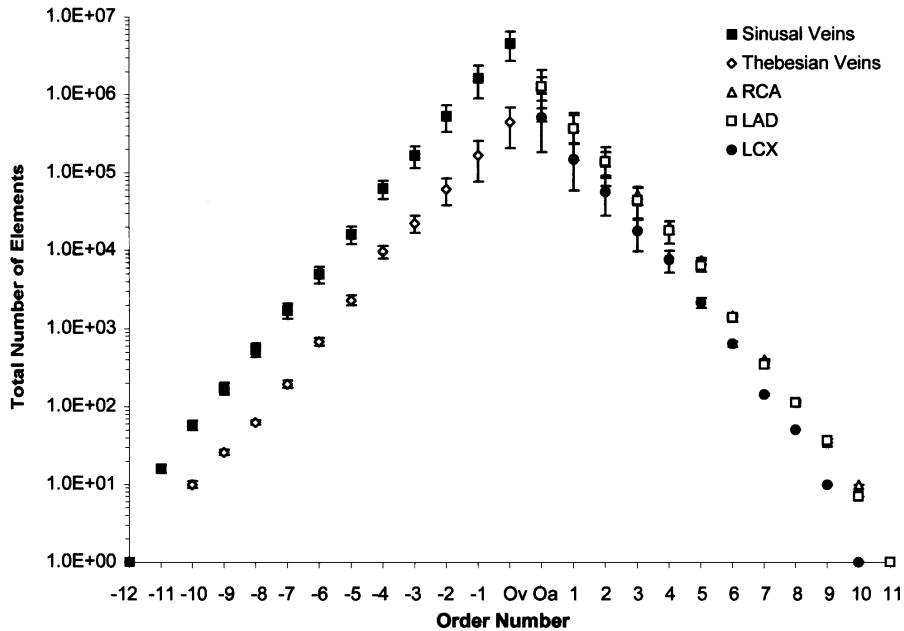


Fig. 5. Relationship between mean total number of vessel elements in successive orders of vessels and order number of vessels in the porcine RCA, LAD, LCx, Thebesian and Sinusal Veins. From Kassab *et al.* (1993a, 1994b), by permission.

the order $-1, -2, -3, \dots, -n, \dots$. Once the entire coronary arterial and venous trees are assigned order numbers, we define those vessel segments of the same order connected in series as elements. Figures 3, 4 and 5 show the relationship between the diameter or major axes length, element length and number of vessels and order number, respectively.

The connectivity of the various elements is presented in the form of a matrix, the component of which in row n and column m are the ratio of the total number of elements of order n sprung from elements of order m , divided by the total number of elements in order m . We call the results the *connectivity matrix* (Kassab *et al.*, 1993a, 1994b). Finally, the longitudinal position matrix of the coronary vasculature is determined, the component of which in row m and column n is the fractional longitudinal position of the vessels of order m which spring directly along the length of vessels of order n . We call the results the *longitudinal position matrix* (Kassab *et al.*, 1997a). In summary, the order number, diameter, length, connectivity matrix, longitudinal position matrix and fractions of the vessels connected in series were measured for all orders of vessels of the right coronary artery (RCA), left anterior descending artery (LAD), left circumflex artery (LCx), coronary sinus and Thebesian veins.

5. Mathematical Description of Capillary Network

We have previously emphasized that the capillary vessels have a non-tree-like branching pattern (Kassab and Fung, 1994). As mentioned above, we designated the capillaries as blood vessels of order number zero; we further designated those capillaries fed directly by

arterioles as C_{0a} , those drained into venules as C_{0v} , and those capillary vessels connected to C_{0a} and C_{0v} as C_{00} (Kassab and Fung, 1994). The capillaries are connected in patterns geometrically identified as Y , T , H or HP (hairpin) and anastomosed through transverse capillary cross-connections (C_{cc}). The C_{cc} vessels may connect adjacent capillaries or capillaries originating from different arterioles.

6. Hemodynamic Applications of Morphometric Data

6.1. Analysis of total cross-sectional area and blood volume

The data on the diameters, lengths, and number of elements can be used to compute the total cross-sectional area (CSA) and blood volume in the coronary arteries or veins. The total CSA , A_n , is equal to the product of the area of each element and the total number of elements:

$$A_n = (\pi/4)D_n^2 N_n \quad (1a)$$

for arteries. The veins have a noncircular cross-sectional area which can be approximated by an ellipse with major and minor axis a and b , respectively (Kassab *et al.*, 1994b). Hence, the CSA for the veins can be expressed as

$$A_n = (\pi/4)a_n^2(b/a)_n. \quad (1b)$$

The total blood volume in all elements of a given order, V_n , are given by

$$V_n = A_n L_n. \quad (2)$$

The cumulative volume of the whole coronary artery or vein is the summation of V_n over n from 1 to N where N is the order of the largest vessel.

6.2. Pressure and flow distributions

6.2.1. Arterial tree

The branching pattern of the coronary arterial tree is prescribed by the connectivity and longitudinal position matrices while the vascular geometry is prescribed by the morphometric data (diameters and lengths). After the branching pattern and vascular geometry of the asymmetric network is generated, a hydrodynamical analysis can be performed (Kassab *et al.*, 1997a, 1997b). The Reynolds' and Womersley's numbers are small in most coronary vessels; hence, the physical laws governing blood flow reduce to Poiseuille's Law which applies for an analysis of steady flow of blood in the coronary vasculature in diastole. We shall initially use Poiseuille's Law to compute the pressure drop across individual vessels, which assumes that the vessels are rigid (the distensibility of the vessels will be considered later). Poiseuille flow, the volumetric flow Q_{ij} , in a vessel between any two nodes, represented by i and j , is given in terms of the pressure differential, ΔP_{ij} , and vessel conductance, G_{ij} , by

$$Q_{ij} = (\pi/128)\Delta P_{ij}G_{ij} \quad (3)$$

where $\Delta P_{ij} = P_i - P_j$, $G_{ij} = D_{ij}^4 \mu_{ij} / L_{ij}$ and D_{ij} , L_{ij} and μ_{ij} are the diameter, length and viscosity, respectively, between nodes i and j . We assume that the coefficient of viscosity

is 4.0 *cp* in vessels of order 11 to 5 and decreases linearly with order number to a value of 2.0 *cp* in the pre-capillary arteriole (Zhuang *et al.*, 1983). There are two or more vessels that emanate from the *j*th node anywhere in the tree with the number of vessels converging at the *j*th node being *m_j*. By conservation of mass we must have

$$\sum_{i=1}^{m_j} Q_{ij} = 0 \tag{4}$$

where the volumetric flow into a node is considered positive and flow out of a node is negative for any branch. From Eqs. (3) and (4) we obtain a set of linear algebraic equations in pressure for *M* nodes in the network, namely

$$\sum_{i=1}^{m_j} [P_i - P_j] G_{ij} = 0. \tag{5a}$$

The set of equations represented by (5a) reduce to a set of simultaneous linear algebraic terms for the nodal pressures once the conductances are evaluated from the geometry, and suitable boundary conditions are specified. The boundary conditions are as follows:

$$\begin{aligned} P(\text{at the Sinus of Valsalva}) &= 100 \text{ mmHg.} \\ P(\text{at the first bifurcation of the capillary network}) &= 26 \text{ mmHg.} \end{aligned} \tag{5b}$$

In matrix form, this set of equations is

$$GP = G'P' \tag{6}$$

where *G* is the *n* × *n* matrix of conductances, *P* is a 1 × *m* column vector of the unknown nodal pressures, and *G'P'* is the column vector of the boundary pressures times the conductances of their attached vessels. The solution to Eq. (6) is obtained in the form of a column vector of the nodal pressures throughout the arterial network. The pressure drops, as well as the corresponding flows, are then computed.

Once the hemodynamics of the network have been determined, Poiseuille's hypothesis can be reexamined. Poiseuille's Law applies only when the flow has a low Reynolds' and Womersely's numbers. The former is defined by the formula *UD/ν* where *U* is the mean velocity of flow, *D* is the blood vessel lumen diameter and *ν* is the kinematic viscosity of blood. The latter is defined as $(D/2)(\omega/\nu)^{1/2}$, where *w* is the circular frequency of pulsatile flow and is computed for a heart rate of 110 cycles/minute. We have previously shown that the Reynolds' number is less than 120 for all orders of vessels and hence justifies the steady state assumption (Kassab *et al.*, 1997b). Womersley's number, on the other hand, is less than 1 for all orders less than 9 (Kassab *et al.*, 1997b). Hence, the inertia of blood should be taken into account for the first several largest orders. Equation (3) may also be corrected for loss due to bifurcation by replacing *m* with the "apparent" viscosity which depends on the Reynolds number. To account for the effect of change of kinetic energy along the stream, at each junction of vessels of order *n* to a vessel of order *n + 1*, a static pressure drop equal to $1/2[\rho U_{n+1}^2 - \rho U_n^2]$ should be added according to the well-known Bernoulli's equation (Fung, 1997) where *U_n* is the mean velocity of flow in the vessel of order *n*.

6.2.2. Capillary network

We have previously stressed that the topological structure of the coronary arteries and intramyocardial veins are tree-like, but the coronary capillary blood vessels have a non-tree-like topology (Kassab *et al.*, 1993a; Kassab and Fung, 1994; Kassab *et al.*, 1994). The analysis of blood flow in the capillaries needs a different network analysis from that presented above. The capillaries not only branch but also cross-connect along their lengths (Kassab and Fung, 1994). The presence of cross-connections in the myocardial capillaries may make the pressure and flow distributions in the capillary bed more uniform and hence must be taken into account when modeling its hemodynamics. The arterial analysis presented is valid for the flow into the capillary network. The capillary network is then simulated based on its geometry, branching pattern, distensibility and blood rheology.

At the capillary dimension, the particulate nature of the blood cells becomes important and the blood properties become non-Newtonian. The viscosity in Poiseuille's law [Eq. (3)] is no longer constant and should be considered as an apparent viscosity, μ_{app} . An empirical formula for the apparent viscosity which accounts for the non-Newtonian properties of blood is (Schmid-Schonbein, 1988)

$$\mu_{\text{app}} = [k_1 + k_2(U/D)^{-1/2}]^2 \quad (7)$$

where U is the mean velocity of blood and D is the diameter of the capillary vessel. The constants k_1 and k_2 depend on vessel diameter, hematocrit and shear rate. The constants have been experimentally determined in rigid glass tubes (Lingard, 1979) and *in vivo* viscosity measurements by Lipowsky *et al.* (1978).

6.2.3. Venous tree

The morphology and connectivity of the venous trees have been presented by Kassab *et al.* (1994b, 1997a). The venous trees are connected to the capillaries as specified by their connectivity matrix. The tree simulations developed above will be applicable to the venous trees with its appropriate vascular connectivity, longitudinal position of bifurcations, vascular geometry, distensibility and boundary conditions. Hence, the hemodynamics of the entire coronary vasculature will be synthesized to determine the pressure-flow relationship of the coronary circulation.

Let us consider some of the hemodynamic modifications needed for the coronary venules and veins because of their unique geometry. Unlike coronary arterioles and arteries which have cylindrical cross-sections, the venules have approximately elliptical cross-sections. If the cross-section of a vein is approximated by an ellipse, then, relative to a set of rectangular Cartesian coordinates x, y with origin located at the center, the parametric equations of the ellipse with a semi-major axis a and a semi-minor axis b are

$$x = a \cos \theta, \quad y = b \sin \theta. \quad (8)$$

The parameters relevant to the flow can be derived from the Navier–Stokes equation. For a steady longitudinal flow of a Newtonian viscous fluid in a long cylindrical tube of elliptic cross-section subjected to a constant pressure gradient, dp/dx . In analogy to the exact solution of flow in a circular cylinder, the velocity profile

$$u = 2U[1 - (x/a)^2 - (y/b)^2] \quad (9)$$

satisfies the Navier-equation and the boundary condition that $u = 0$ on the elliptic wall described by Eq. (8). U is the mean velocity over this section. With Eq. (9), the Navier–Stokes equation yields

$$dP/dx = -4\mu U[(a^2 + b^2)/(a^2b^2)] \quad (10)$$

where μ is the coefficient of viscosity of the fluid, and x is the length along the longitudinal axis of the tube. Then the volume rate of flow is

$$Q = \text{Area} U = \pi abU = \pi/4\mu L[(a^3b^3)/(a^2 + b^2)]dP/dx. \quad (11)$$

The resistance to flow is given by:

$$\text{Resistance} = 4\mu L/\pi[(a^2 + b^2)/(a^3b^3)] \quad (12)$$

where L is the length of the tube. The formulas (9)–(12) show that a and the ratio b/a are the most important parameters of venous blood flow in which the Womersley number is less than one and have been measured in detail (Kassab *et al.*, 1994).

7. Distensibility of Coronary Vessels

Vessel distensibility data are necessary because the elasticity of blood vessels of an organ is an important determinant of the pressure-flow relationship of blood flow through the organ. Pressure affects blood vessel diameter which, in turn, controls pressure distribution. Mathematically, the hemodynamic equations consist of an equation describing blood motion, and an equation for blood vessel deformation. The interaction of the two equations enters through the boundary conditions.

We have recently obtained data on the distensibility of the coronary vessels in the form of a pressure-diameter relation (unpublished data). Our data show two important features of distensibility of coronary arteries: (1) that the relationship is linear in the physiological range of pressures and (2) the compliance is small; i.e. the coronary epicardial arteries are relatively rigid in the diastolic state of the heart.

8. Steady Laminar Flow in an Elastic Tube

With the distensibility of the blood vessels known, the mechanics of the blood vessel is coupled to the mechanics of blood flow to yield a pressure-flow relation for each vessel segment. This can be demonstrated for the cylindrical coronary arteries as follows: assume that the tube is long and slender, that the flow is laminar and steady, that the disturbances due to entry and exit are negligible, and that the deformed tube remain smooth and slender. These assumptions permit the use of Poiseuille's law for a Newtonian fluid that can be state as

$$dP/dx = (128\mu/\pi D^4)Q \quad (13)$$

where P is the pressure, x is the axial coordinate, Q is the volume-flow rate and D , and μ are the diameter, and viscosity, respectively. In a stationary, nonpermeable tube Q is a constant throughout the length of the tube. The tube diameter is a function of x because

of the elastic deformation. Our data shows that, in the physiological pressure range, the elastic deformation can be described by the equation

$$D - D^* = \alpha(P - P^*) \quad (14)$$

where D is the diameter at a given intravascular pressure P , D^* is the diameter corresponding to a pressure P^* and α is the compliance constant of the vessel. Using Eq. (14), we have

$$dP/dx = dP/dD dD/dx = 1/\alpha dD/dx. \quad (15)$$

On substituting Eq. (14) into Eq. (13) and rearranging terms, we obtain

$$D^4 dD = (128\mu\alpha Q/\pi) dx. \quad (16)$$

Since the right-hand side term is a constant independent of x , we obtain the integrated result

$$D^5(x) = (640\mu\alpha Q/\pi)x + D^5(0). \quad (17)$$

The integration constant can be determined by the boundary condition, at the entry section of the vessel, that when $x = 0$, $D(x) = D(0)$. Putting $x = L$, at the exit section of a vessel, in Eq. (17) yields

$$D^5(L) - D^5(0) = 640\mu\alpha QL/\pi. \quad (18)$$

We now seek an approximate expression of Eq. (18) when $D(L) - D(0)$ is small; i.e. the vessel compliance is small. Letting $D(L) = D(0) + \varepsilon$, expanding the left hand side of Eq. (18) in power series of ε , and retaining only terms up to ε^2 , we obtain the approximation

$$[D(L) - D(0)]\{1 + 2[D(L) - D(0)]/D(0)\} = (128\mu\alpha LQ)/(\pi D^4(0)). \quad (19)$$

Using Eq. (14) first at $x = L$ and then at $x = 0$ and subtracting, we have

$$D(L) - D(0) = \alpha[P(L) - P(0)]. \quad (20)$$

Combining (19) and (20), and writing D_0 for $D(0)$, we obtain

$$\Delta P + (2\alpha/D_0)\Delta P^2 = (128\mu LQ/\pi D_0^4) \quad (21)$$

where $\Delta P = P(L) - P(0)$. The solution to Eq. (21) takes the form

$$\Delta P_n = [-D_n + (D_n^2 + 8\alpha_n \Delta P_{pn} D_n)^{1/2}]/4\alpha_n \quad (22)$$

where ΔP_p is the Poiseuille's pressure drop as given by the right hand side of Eq. (21) and applies to each arterial vessel of order n . The pressure drop in Eq. (22) can be plotted as a function of the compliance α for the various orders of arterial vessels as shown in Fig. 6. It can be seen that when the compliance is zero (rigid vessel), the pressure drop corresponds to that given by Poiseuille's equation. However, when the compliance is nonzero, the pressure drop is smaller than that given by Poiseuille's equation and varies for different orders of vessels.

In the case of a non-Newtonian blood, as in the capillary vessels, the hydrodynamic law [Eq. (13)] can be combined with the elasticity [Eq. (14)] and rheology of blood [Eq. (7)] relationships to yield

$$dP/dx = (128/\pi)[k_1 + k_2[\pi(\alpha(P - P^*) + D^*)^3/4Q]^{1/2}]^2[\alpha(P - P^*) + D^*]^{-4}Q. \quad (23)$$

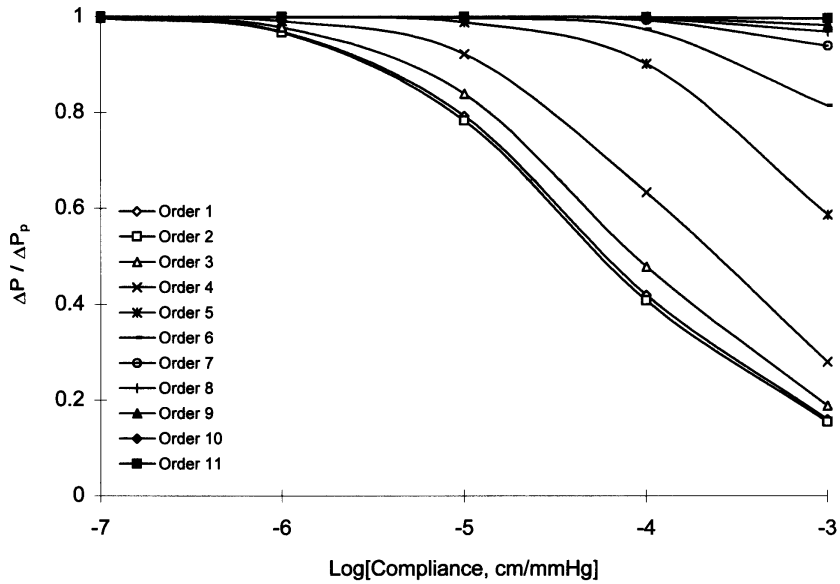


Fig. 6. Relationship between normalized pressure drop and logarithm of compliance constant for various orders of the left common coronary artery.

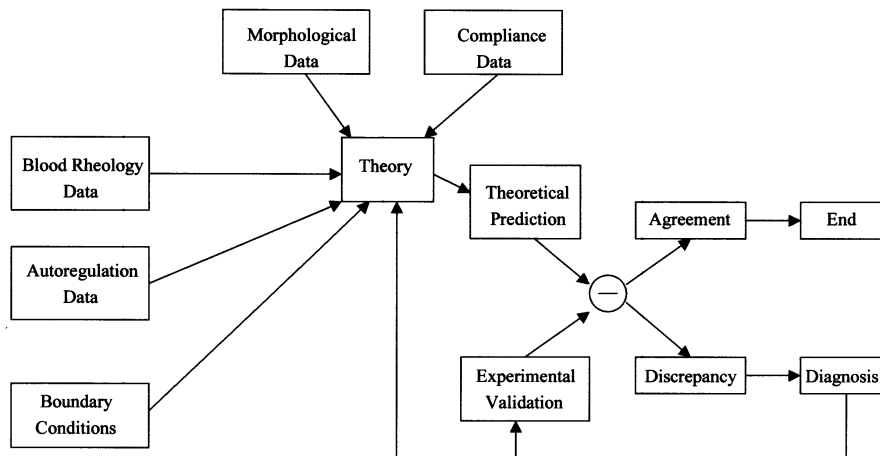


Fig. 7. A block diagram showing the interaction between input data (morphological, compliance, etc.), theoretical predictions and experimental validations.

This is the governing equation for non-Newtonian viscous blood flow in an elastic vessel at steady state conditions which can be integrated for specific boundary conditions (Kassab *et al.*, 1999).

9. Integration of Theory and Experiment

The interaction of the anatomy, elasticity, vasoactivity, tissue/vessel interaction, theoretical analysis and experimental validation is presented in Fig. 7. When the theoretical and

experimental results are compared, one may find that they do agree. In that case the process ends successfully and one gains confidence in the theory, which can then be used to predict the behavior of the physiological system. On the other hand, one may find that they disagree. Then it is necessary to examine carefully the cause of the discrepancy. With the diagnosis, one may wish to improve the experiment, or the theory, or both. With the improved theory and experiment, the process is repeated. The iterative process ensues until there is agreement between theory and experiment. This second alternative is what usually happens and provides real opportunity for learning and discovery.

10. Concluding Remarks

A mathematical model of coronary circulation should be constructed based on the physical laws governing blood flow, the set of measured data on anatomy and elasticity of the coronary blood vessels, data on muscle/vessel interaction and vasoactivity, rheology of blood and the appropriate boundary conditions. This yields a predictive model that incorporates some of the factors controlling coronary blood flow. The virtue of the model will be determined through experimental validation. The model of normal hearts will serve as a physiologic reference state. Pathological states can then be studied in relation to changes in model parameters that alter coronary perfusion. This chapter illustrates the use of physical principles, with the help of anatomy and mechanical properties, to explain and predict the physiology of the coronary circulation in quantitative terms.

In this chapter, I hoped to demonstrate the extent to which an engineering approach can yield precise information about the blood circulation in the heart. The theory connects a large number of physical, morphometric, and rheological variables. Without such an approach, it would be very difficult to correlate all of these variables by conventional, empirical methods. In the present research, we are building our theory on continuum mechanics, and using measured geometric and elasticity data. *Ad hoc* hypotheses are kept to a minimum. Hence, the theory is basic and the agreement between the theoretical predictions and experimental results will yield conviction in the usefulness of the engineering approach.

References

1. Fung, Y. C., *Biomechanics: Circulation*, Springer Verlag, New York (1997).
2. Hoffman, J. I. E. and Spann, J. A. E., Pressure-flow relations in the coronary circulation, *Physiol. Rev.* **70**, 331–390 (1990).
3. Kassab, G. S. and Fung, Y. C., The pattern of coronary arteriolar bifurcations and the uniform shear hypothesis, *Ann. Biomed. Eng.* **23**, 13–20 (1995).
4. Kassab, G. S. and Fung, Y. C., Topology and dimensions of the pig coronary capillary network, *Am. J. Physiol.* **267** (Heart Circ. Physiol. 36), H319–H325 (1994).
5. Kassab, G. S., Rider, C. A., Tang, N. J. and Fung, Y.-C. B., Morphometry of pig coronary arterial trees, *Am. J. Physiol.* **265** (Heart Circ. Physiol. 34), H350–H365 (1993a).
6. Kassab, G. S., Lin, D. and Fung, Y. C., Consequences of pruning in morphometry of coronary vasculature, *Ann. Biomed. Eng.* **22**, 398–403 (1994a).

7. Kassab, G. S., Lin, D. and Fung, Y. C., Morphometry of the pig coronary venous system, *Am. J. Physiol.* **267** (Heart Circ. Physiol. 36), H2100–H2113 (1994b).
8. Kassab, G. S., Pallencaoe, E. and Fung, Y. C., The longitudinal position matrix of the pig coronary artery and its hemodynamic implications, *Am. J. Physiol.* **273** (Heart Circ. Physiol. 42) H2832–H2842 (1997a).
9. Kassab, G. S., Berkley, J. and Fung, Y. C., Analysis of pig's coronary arterial blood flow with detailed anatomical data, *Ann. Biomed. Eng.* **25**, 204–217 (1997b).
10. Kassab, G. S., Imoto, K., White, F. C., Rider, C. A., Fung, Y.-C. B. and Bloor, C. M., Coronary arterial tree remodeling in right ventricular hypertrophy, *Am. J. Physiol.* **265** (Heart Circ. Physiol. 34), H366–H375 (1993b).
11. Kassab, G. S., K. N. Le and Y. C. Fung, A hemodynamic analysis of coronary capillary blood flow based on anatomic and distensibility data. *Am. J. Physiol.* 277 (Heart Circ. Physiol. 46): H2158–H2166, (1999).
12. Oh, B.-H., Volpini, M., Kambayashi, M., Murata, K., Rockman, H., Kassab, G. S. and Ross, J. R., *Circulation* **86**, 1265–1279 (1992).
13. Schmid-Schoenbein, G. W., A theory of blood flow in skeletal muscle, *J. Biomech. Eng., Trans. ASME* **110**, 20–26 (1986).
14. Zhuang, F. Y., Fung, Y. C. and Yen, R. T., Analysis of blood flow in cat's lung with detailed anatomical and elasticity data, *J. Appl. Physiol.: Respirat. Environ. Exercise Physiol.* **55**, 1341–1448 (1983).